Colloids and Surfaces B: Biointerfaces 199 (2021) 111540

Contents lists available at ScienceDirect

Colloids and Surfaces B: Biointerfaces

journal homepage: www.elsevier.com/locate/colsurfb

Direct electrochemistry of covalently immobilized hemoglobin on a naphthylimidazolium butyric acid ionic liquid/MWCNT matrix

Manoharan Murphy, K. Theyagarajan, Kathavarayan Thenmozhi *, Sellappan Senthilkumar *

Department of Chemistry, School of Advanced Sciences, Vellore Institute of Technology (VIT), Vellore, 632014, India

ARTICLE INFO

Keywords:
Hydrogen peroxide
Ionic liquid
Hemoglobin
Direct electrochemistry
Biosensor

ABSTRACT

Monitoring the concentration levels of hydrogen peroxide (H_2O_2) is significant in both clinical and industrial applications. Herein, we develop a facile biosensor for the detection of H_2O_2 based on direct electron transfer of hemoglobin (Hb), which was covalently immobilized on a hydrophobic naphthylimidazolium butyric acid ionic liquid (NIBA-IL) over a multiwalled carbon nanotube (MWCNT) modified glassy carbon electrode (GCE) to obtain an Hb/NIBA-IL/MWCNT/GCE. Highly water-soluble Hb protein was firmly immobilized on NIBA-IL via stable amide bonding between the free —NH_2 groups of Hb and —COOH groups of NIBA-IL via EDC/NHS coupling. Thus fabricated biosensor showed a well resolved redox peak with a cathodic peak potential (E_{pc}) at −0.35 V and anodic peak potential (E_{pa}) at −0.29 V with a formal potential ($E^{\circ\prime}$) of −0.32 V, which corresponds to the deeply buried Fe^{III}/Fe^{II} redox centre of Hb, thereby direct electrochemistry of Hb was established. Further, the modified electrode demonstrated very good electrocatalytic activity towards H_2O_2 reduction and showed a wide linear range of detection from 0.01 to 6.3 mM with a limit of detection and sensitivity of 3.2 μM and 111 μA mM^{-1} cm^{-2}, respectively. Moreover, the developed biosensor displayed high operational stability under dynamic conditions as well as during continuous potential cycles and showed reliable reproducibility. The superior performance of the fabricated biosensor is attributed to the effective covalent immobilization of Hb on the newly developed highly conducting and biocompatible NIBA-IL/MWCNT/GCE platform.

1. Introduction

Hydrogen peroxide (H_2O_2) is an essential oxidizing and reducing agent and plays a vital role in pharmaceutical, food manufacturing, textile, mining, clinical and environmental applications [1–3]. Moreover, H_2O_2 is involved in several biological and biochemical processes in living organism especially apoptosis, immune cell activation, stomatal closure, vascular remodelling and enzyme catalysis [4]. It is well known that a high concentration of H_2O_2 (>millimolar levels) in cell proliferation will lead to various types of diseases in the body, such as cancer, Parkinson's disease, Huntington's disease, Alzheimer's disease and neurodegenerative disorders [5,6]. In view of this, the determination of H_2O_2 concentration is of practical significance in both healthcare and environmental sector as well. Therefore, there is a crucial need to develop cost-effective, rapid, sensitive and selective H_2O_2 sensors. So far, various analytical methods such as titrimetry, chemiluminescence, high performance liquid chromatography, fluorescence, colorimetry and electrochemical methods have been employed to monitor H_2O_2 concentrations [7–11]. Among them, electrochemical determination of H_2O_2 stands superior owing to its easy operation, good sensitivity, selectivity, simple instrumentation and extendable for real-time analysis [12–14].

The electrochemical determination of H_2O_2 could be performed either enzymatically or non-enzymatically. Many researchers have made substantial efforts in designing materials for the non-enzymatic sensing of H_2O_2 [15,16], however these non-enzymatic sensors often result in insufficient selectivity. To accomplish good selectivity, sensitivity and reproducibility, enzymatic sensors can be used as an appreciable probe for the determination of H_2O_2 owing to the rapid biocatalytic reactions of the biological recognition element. In this respect, heme containing proteins and enzymes including myoglobin, cytochrome c, horseradish peroxidase and hemoglobin (Hb) are widely used in quantification of H_2O_2 [17–19]. Among them, Hb plays an important role as an oxygen carrier and the iron present in porphyrin ring can undergo several redox reactions essential for the biological process of organisms. Further, Hb has the potential to be incorporated in an electrochemical biosensor to study the electrocatalytic behaviour of many analytes. Interestingly, Hb exhibits peroxidase like activity and hence Hb based biosensors are

* Corresponding authors.
E-mail addresses: k.thenmozhi@vit.ac.in, kt.thenmozhi@gmail.com (K. Thenmozhi), senthilkumar.s@vit.ac.in, senthilanalytical@gmail.com (S. Senthilkumar).

https://doi.org/10.1016/j.colsurfb.2020.111540
Received 30 April 2020; Received in revised form 3 December 2020; Accepted 12 December 2020
Available online 29 December 2020

commonly used for the quantitative detection of H_2O_2. However, the direct electron transfer (DET) between heme redox centre and electrode surface is more complicated as the active iron centre are deeply embedded in non-conductive dense polypeptide chain [20]. To circumvent this communication issue and to facilitate the DET, different kinds of materials including nanoparticles, biopolymers, bio-membranes and surfactants, possessing large surface area, tunable porosity, biocompatibility and higher conductivity are continuously being explored [21].

Ionic liquids (ILs) have been widely used in the fabrication of electrochemical sensors and biosensors due to their excellent properties such as superior ionic conductivity (>30 mS cm^{-1}), a wide electrochemical window (up to 5.0 V), tuneable viscosity and biocompatibility [22,23]. Functionalized ILs are a class of ILs with appropriate functionality designed for task-specific applications [24,25]. Different functionalised ILs with hydroxyl (—OH), amine (NH_2), aldehyde (—CHO), sulfonic acid (—SO_3H), thiol (—SH) and nitrile (—C≡N) groups have been synthesized and utilized for various applications in their respective fields [26, 27]. Meanwhile, platforms with carboxyl functionality (—COOH) have received significant attention in electrochemical biosensors for covalent immobilization of biomolecules through amide bond formation [28]. Thus, we have developed a phosphonium based IL comprising carboxyl functional group and employed towards immobilization of cytochrome *c* [29]. However, the phosphonium IL affords limited synthetic versatility, which motivated us to design ILs with tailor-made features to ensure firm immobilization and enhanced electrical communication. Meanwhile, imidazolium based ILs have received great attention due to their π-conjugated heterocyclic five-membered ring system and these ILs offer excellent synthetic versatility and tuneable physicochemical properties. Accordingly, we sought to prudently design an imidazolium IL with naphthyl substitution and also carboxyl functional groups for the effectual immobilization of Hb.

In the present work, naphthylimidazolium butyric acid ionic liquid (NIBA-IL) was synthesized and immobilized on a multiwalled carbon nanotube coated glassy carbon electrode (MWCNT/GCE) to afford NIBA-IL/MWCNT/GCE as a novel and effective platform for the immobilization of biomolecules. In this work, a carboxylic acid functionalised IL will be used for the covalent immobilization with amine groups of Hb protein. Further, naphthyl group of IL with extensive π-electron cloud would aid the firm immobilization on the MWCNT/GCE via π–π stacking, and the IL form of the molecule would render high conductivity for the system and biocompatible microenvironment for Hb protein [30]. MWCNTs would provide augmented electronic conductivity along with IL to facilitate the DET of deeply embedded Fe^{III}/Fe^{II} redox centre of Hb. The modified electrode is fabricated by immobilizing Hb on NIBA-IL based platform through stable amide bond formation using 1-ethyl-3-(3-dimethylaminopropyl)carbodiimide hydrochloride (EDC)/N--hydroxysuccinimide (NHS) coupling reaction to form a Hb/NIBA-IL/MWCNT/GCE. The proposed biosensor was electrochemically characterized using cyclic voltammetry and distinct redox peak corresponding to the redox couple of Hb (Fe^{III}/Fe^{II}) was observed. Further, the electrocatalytic efficacy of the modified electrode towards determination of H_2O_2 under static and dynamic condition was investigated and the biosensor exhibited a wide linear range with good sensitivity and low detection limits. Also, the fabricated biosensor has shown excellent selectivity, stability and reproducibility towards H_2O_2 determination.

2. Experimental

2.1. Chemicals and materials

Hemoglobin porcine (lyophilized powder), 1-naphthaleneacetic acid (≥95 %), 1-(3-aminopropyl) imidazole (97 %), 4-bromobutyric acid (98 %), bis(trifluoromethane)sulfonimide lithium salt (99.95 %), EDC (≥97 %), NHS (98 %), thionyl chloride (≥99 %), and MWCNTs (>90 % carbon basis) were procured from Sigma-Aldrich, India. All solvents and reagents of analytical grade were used as received. A GCE (CH Instruments, USA) with a geometric area of 0.071 cm^2 was used as the working electrode. In our work, 0.1 M phosphate buffer (pH 7.0) was employed as the supporting electrolyte, which was prepared by mixing NaH_2PO_4 and Na_2HPO_4. EDC/NHS solutions were prepared using the 0.1 M phosphate buffer (pH 7.0). All aqueous solutions used in electrochemical measurements were prepared using Milli-Q water (18.2 MΩ cm at 25 °C).

2.2. Instrumentation

^1H, ^{13}C, ^{19}F Nuclear magnetic resonance (NMR) spectra were recorded using a Bruker spectrometer in DMSO-d_6 and $CDCl_3$ deuterated solvents. Chemical shifts (δ) are stated in parts per million (ppm) downfield from tetramethylsilane (δ=0.00). Fourier-transform infrared (FTIR) spectra were performed in the range between 4000 and 400 cm^{-1} on an IR Affinity-1, Shimadzu spectrophotometer. UV–vis absorption spectra were recorded on a JASCO spectrophotometer (V-670 PC) in the wavelength range between 200 and 800 nm. High-resolution mass spectra (HRMS) were obtained using an EI JEOL GC Mate-II spectrometer with an electron impact (70 eV) ionisation. All electrochemical experiments were performed using a CHI 760E electrochemical workstation obtained from CH Instruments, USA. A conventional three electrode system, consisting of a modified/unmodified GCE as the working electrode, a Ag|AgCl reference electrode and a platinum wire counter electrode, was used in all electrochemical experiments.

2.3. Synthesis of naphthylimidazolium butyric acid ionic liquid (NIBA-IL)

Synthesis of NIBA-IL was carried out by following steps schematically shown in Fig. 1A. The first step is a classical acid to acid chloride conversion with the help of thionyl chloride. Thereafter, amidation was performed between the formed acid chloride and aminopropyl imidazole in the presence of triethylamine to form the derivative of imidazole. Then it was quaternized with bromobutryic acid to form the bromide based IL, which on metathesis with bis(trifluoromethane)sulfonimide yields NIBA-IL.

2.3.1. Synthesis of 3-(5-carboxypentyl)-1-(3-(2-(naphthalen-1-yl) acetamido)propyl)-imidazol-3-ium bromide

Procedure for the synthesis of 2-(naphthalene-2-yl)acetyl chloride **(1)** and N-(3-(1H-imidazol-1-yl)propyl)-2-(naphthalen-1-yl)acetamide **(2)** and their spectral characterization using ^1H NMR, ^{13}C NMR and FTIR spectroscopy are provided in the supplementary material. Acetonitrile solution (10 mL) of N-(3-(1H-imidazol-1-yl)propyl)-2-(naphthalen-1-yl) acetamide (1.22 g, 41 mmol) was stirred for 1 h at 70 °C. To this, 4-bromobutyric acid (0.69 g, 41 mmol) in acetonitrile (10 mL) was added dropwise for 30 min under constant stirring and continued stirring for another 14 h at 85 °C. After the reaction, the organic layer was filtered off and the resulting crude was washed with ethyl acetate (2 × 20 mL), followed by diethyl ether (2 × 30 mL). Finally, the obtained 3-(5-carboxypentyl)-1-(3-(2-(naphthalen-1-yl)acetamido)propyl)-1H-imidazol-3-ium bromide **(3)** was dried under high vacuum, to give reddish-brown liquid. Yield: 89 %.

2.3.2. Synthesis of Bis(3-(3-carboxypropyl)-1-(3-(2-(naphthalen-1-yl) acetamido)propyl)-imidazol-3-ium) mono(bis((trifluoromethyl)sulfonyl) amide) [NIBA-IL]

3-(5-Carboxypentyl)-1-(3-(2-(naphthalen-1-yl)acetamido)propyl)-1H-imidazol-3-ium bromide (1.0 g, 21 mmol) was dissolved in 15 mL of methanol, to which bis(trifluoromethane)sulfonimide lithium salt (0.6 g, 21 mmol) in methanol (20 mL) was slowly added and the resulting mixture was continuously stirred for 12 h at room temperature. The resultant crude product was washed with diethyl ether (3 × 20 mL) and then dried at 60 °C under vacuum, to give reddish-brown liquid of NIBA-

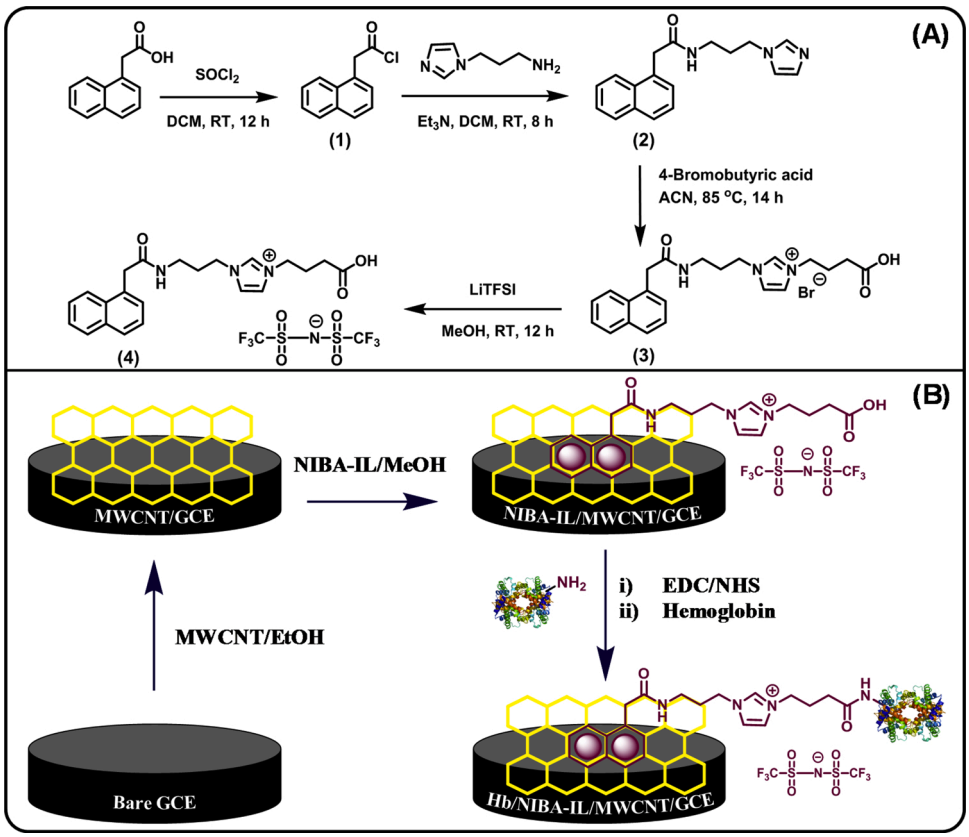

Fig. 1. A) Scheme for the synthesis of NIBA-IL and B) Step-wise fabrication of Hb/NIBA-IL/MWCNT/GCE electrode.

IL **(4)**. Yield: 92 %.

2.4. Fabrication of Hb/NIBA-IL/MWCNT/GCE biosensor

The step-wise modification and covalent anchoring of Hb on NIBA-IL/MWCNT/GCE is shown in Fig. 1B. Initially, the GCE was mirror polished using different grades of alumina slurries and then ultrasonicated in ethanol/water (1:1) mixture for 5 min. Thereafter, 5 μL of MWCNTs (2 mg/mL in ethanol) was drop-casted on a precleaned GCE surface, and it was dried at ambient temperature to form a MWCNT/GCE. To this, 5 μL of NIBA-IL (2 mg/mL in methanol) was drop-casted over MWCNT/GCE to obtain a NIBA-IL/MWCNT/GCE. Further, the carboxyl group on the modified electrode was activated through EDC (0.4 M) followed by NHS (0.1 M) for 1 h each [31]. Finally, the covalent immobilization of Hb on NIBA-IL was done by drop-casting Hb (2 mg/mL in 0.1 M phosphate buffer) on the carboxyl activated electrode to allow the free —NH_2 groups of Hb to react with —COOH groups of NIBA-IL to form a stable amide bond and dried for 1 h to result in Hb/NIBA-IL/MWCNT/GCE. This fabricated electrode was gently washed with phosphate buffer before subjecting for electrochemical studies.

3. Results and discussion

The synthesized hydrophobic NIBA-IL was characterized using ^{1}H, ^{13}C, ^{19}F NMR, FTIR and HRMS spectra and the results are presented in the electronic supplementary information (Figs. S7 – S9).

3.1. Covalent immobilization of Hb on NIBA-IL

Covalent anchoring of Hb on NIBA-IL was confirmed by performing

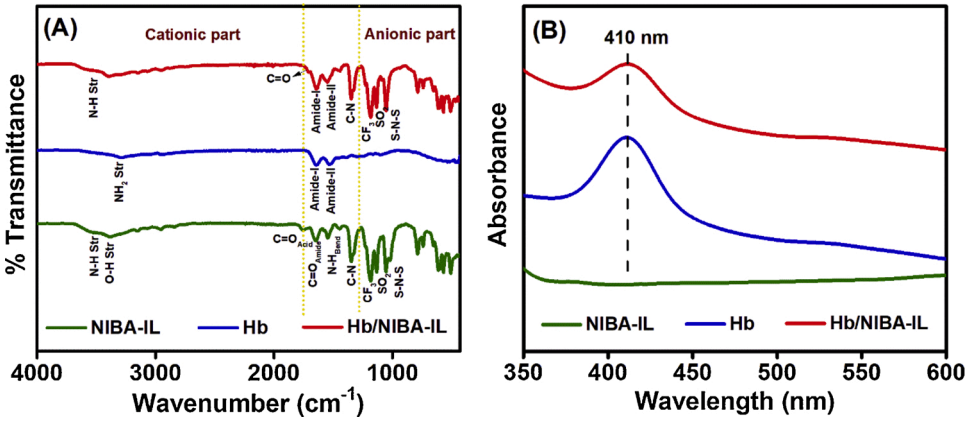

Fig. 2. Comparative A) FTIR and B) UV–vis spectra of NIBA-IL (green), Hb (blue) and Hb/NIBA-IL (red).

FTIR spectral analysis (Fig. 2A) of NIBA-IL (green), Hb (blue), and Hb/NIBA-IL (red). The stretching vibration bands at 3429 and 3241 cm^{-1} are assigned to ν(—NH) and ν(—OH) and the sharp peaks at 1755, 1645, 1164 and 1085 cm^{-1} correspond to ν(—C═O_{Acid}), ν(—C═O_{Amide}), ν(—C—O) and ν(—C—F) groups present in the NIBA-IL [32–34]. The FTIR spectrum of Hb shows two characteristic absorption peaks at 1643 and 1531 cm^{-1} representing the amide I and amide II absorption bands of polypeptide chains present in Hb protein [35]. The covalent immobilization of Hb on NIBA-IL via amide bond formation between the —NH_2 of Hb and —COOH of NIBA-IL was confirmed by the disappearance of ν(—OH) peak of NIBA-IL and formation of new peaks at 3582 and 1723 cm^{-1} due to ν(NH) and ν(—C═O) of amide group respectively. Noteworthily, the amide I and amide II peaks of unmodified Hb were retained with a slight shift in the frequencies in Hb/NIBA-IL and such minor changes neither destroy the structure nor alter the fundamental nature of Hb [36]. These results indicate that the Hb molecules preserve their native state even after being covalently bonded with NIBA-IL. Fig. 2B shows the UV–vis absorption spectra of NIBA-IL (green), Hb (blue), and Hb/NIBA-IL (red). There is no obvious absorption band observed for NIBA-IL, whereas Hb protein displayed the characteristic Soret band around 410 nm. Interestingly, Hb/NIBA-IL also exhibited the Soret band, which indicates that Hb retains its nativity even after covalent anchoring on NIBA-IL and is due to the impressive biocompatibility afforded by the newly designed NIBA-IL [37].

3.2. Electrochemical impedance spectroscopy on Hb/NIBA-IL/MWCNT/GCE

Electrochemical impedance spectroscopy (EIS) is an effective tool to monitor the changes occuring in the electrode/electrolyte interfaces. Fig. 3A shows the Nyquist plots of bare GCE (brown), MWCNT/GCE (orange), NIBA-IL/MWCNT/GCE (green), Hb/NIBA-IL/GCE (red) and Hb/NIBA-IL/MWCNT/GCE (blue) at an applied potential of 0.21 V (formal potential) between the frequency range of 1×10^6 Hz and 0.1 Hz with an AC potential amplitude of 0.01 V in a 0.1 M KCl solution containing 5 mM $[Fe(CN)_6]^{4-/3-}$. The EIS spectrum consists of a semicircle region at lower frequencies and a linear part at higher frequencies and the diameter of the semicircle denotes the charge transfer resistance (R_{ct}). Bare GCE showed a large R_{ct} value of 411 Ω for the electron transfer process that occurs between the electrode surface and $[Fe(CN)_6]^{4-/3-}$ solution. After modifying the bare GCE surface with MWCNTs, the R_{ct} value reduced to 268 Ω, due to the conducting nature of MWCNTs. Further incorporation of NIBA-IL over MWCNT/GCE through π--π stacking, has reduced the R_{ct} value to the lowest of 144 Ω, indicating the high conducting nature of NIBA-IL. Covalent immobilization of Hb on NIBA-IL/GCE significantly increases the R_{ct} value to the maximum of 733 Ω, demonstrating the effective immobilization of non-conducting protein layers that hinder the electron transfer process. Further inclusion of MWCNTs into Hb/NIBA-IL/GCE reduces the R_{ct} to 603 Ω, denoting the synergic behaviour between the NIBA-IL and MWCNTs, which enhances the conductivity of the fabricated biosensor. The EIS results depict the suitability of the newly designed NIBA-IL/MWCNT/GCE platform for the effective fabrication of Hb based biosensor.

3.3. Direct electrochemistry of Hb at Hb/NIBA-IL/MWCNT/GCE

The direct electron transfer of covalently immobilized Hb on NIBA-IL/MWCNT/GCE was demonstrated by performing cyclic voltammetry in N_2 saturated 0.1 M phosphate buffer at a scan rate of 100 mV s^{-1} and the cyclic voltammograms of step-wise fabrication of Hb/NIBA-IL/MWCNT/GCE is shown in Fig. 3B. The cyclic voltammograms at a bare GCE (brown), a MWCNT/GCE (orange) and a NIBA-IL/MWCNT/GCE (green) did not exhibit any redox peak in the potential range of 0.1 V to −0.8 V, which indicates the non-redox behaviour of these modified electrodes within the potential window studied. Cyclic voltammogram at a Hb/MWCNT/GCE (in the absence of NIBA-IL) resulted in a highly unstable response (figure not shown), which shows that immobilization of Hb occurs only through NIBA-IL and not on MWCNTs. Noticeably, the Hb/NIBA-IL/GCE (red) showed a set of redox peaks with a cathodic peak potential (E_{pc}) at −0.366 V and an anodic peak potential (E_{pa}) at −0.304 V to yield a formal potential ($E^{\circ\prime}$) of −0.335 V, and the obtained $E^{\circ\prime}$ is in accordance with that of the immobilized Hb ($E^{\circ\prime}$ of −0.338 V) reported earlier [38]. As shown in Eq. (1), the redox active heme site (Fe^{III}/Fe^{II}) of Hb undergoes a reversible one electron redox process with a ΔE_p of 62 mV. These results indicate that the newly designed NIBA-IL could effectively communicate with the deeply buried redox centre of Hb, due to the highly conducting and biocompatible nature of NIBA-IL. Further, inclusion of MWCNTs on the electrode platform (Hb/NIBA-IL/MWCNT/GCE, blue) enhances both the anodic and cathodic peak currents by ~45 %, as well as decreases the $E^{\circ\prime}$ to −0.325 V (with a E_{pc}, E_{pa} and ΔE_p of −0.356 V, −0.294 V and 62 mV, respectively). The increase in peak currents is due to the increase in surface area of the modified electrode in the presence of MWCNTs and the decrease in formal potential is accredited to the enhanced conductivity through synergic behaviour of NIBA-IL and MWCNTs.

$$\text{Hb-Heme } (Fe^{III}) + e^- \rightarrow \text{Hb-Heme } (Fe^{II}) \quad (1)$$

Cyclic voltammetry of 0.1 M phosphate buffer (pH 7.0) was conducted at the Hb/NIBA-IL/MWCNT/GCE at potential scan rate ranging from 5 to 500 mV s^{-1} and the results obtained are shown in Fig. 4. On increasing the scan rate, the anodic and cathodic peak currents gradually increased without any significant change in peak potentials and the plot of peak current against square root of scan rate showed a linear

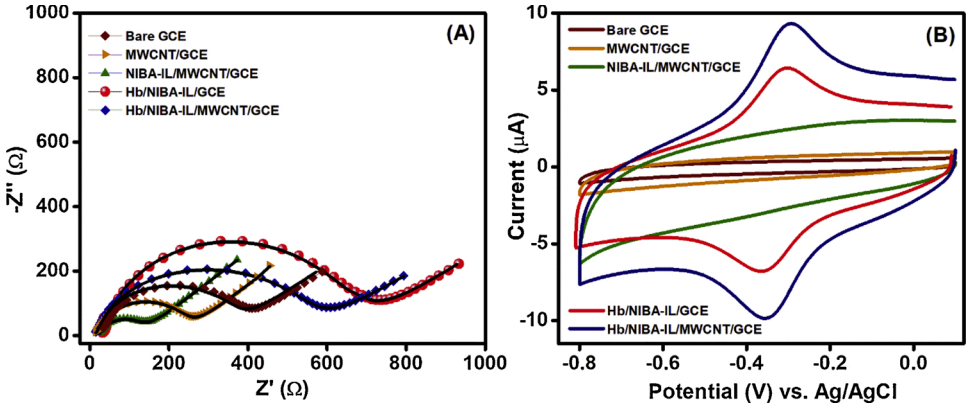

Fig. 3. A) Nyquist plot in 0.1 M KCl solution containing 5 mM $Fe(CN)_6^{3-/4-}$ and B) Cyclic voltammograms at a bare GCE (brown), MWCNT/GCE (orange), NIBA-IL/MWCNT/GCE (green), Hb/NIBA-IL/GCE (red), and Hb/NIBA-IL/MWCNT/GCE (blue) at a scan rate of 100 mV s^{-1} in N_2 saturated 0.1 M phosphate buffer (pH 7.0).

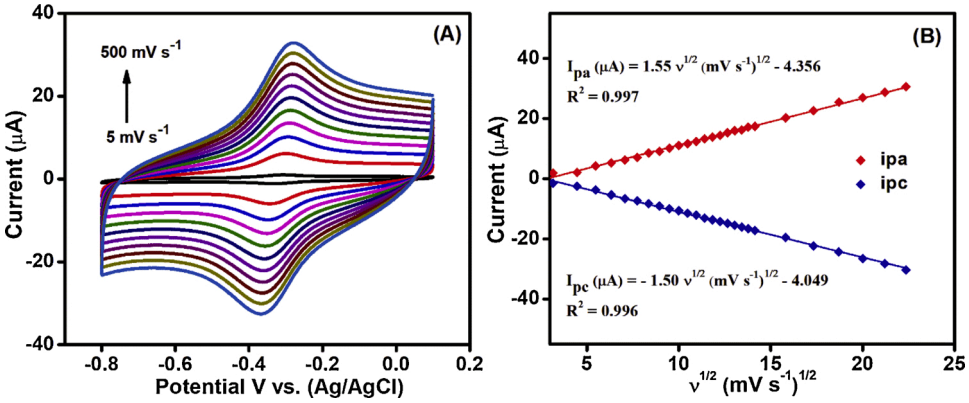

Fig. 4. A) CVs of 0.1 M phosphate buffer (pH 7.0) at a Hb/NIBA-IL/MWCNT/GCE at different scan rates from 5 mV s^{-1} to 500 mV s^{-1}. B) Linear plot of peak current versus square root of scan rate.

trend, indicative of a diffusion-controlled process. The effect of electrolyte pH on Hb/NIBA-IL/MWCNT/GCE was studied in 0.1 M phosphate buffer of varying pH from 4 to 10 and the fabricated biosensor exhibited better electrochemical behaviour at neutral pH 7.0. The maximum cathodic peak current (9.9 μA) obtained at neutral pH could be due to the favourable biological microenvironment for the immobilized Hb, which preserves its activity and enhances its performance (Fig. S10).

3.4. Electrocatalytic reduction of H_2O_2 at Hb/NIBA-IL/MWCNT/GCE

The electrocatalytic efficacy of the developed Hb biosensor towards reduction of H_2O_2 was investigated by cyclic voltammetry with varying concentrations of H_2O_2 in 0.1 M phosphate buffer. Fig. 5A shows the cyclic voltammograms of 0.0, 1.0, 2.0 and 3.0 mM H_2O_2 at a Hb/NIBA-IL/MWCNT/GCE at a scan rate of 100 mV s^{-1}. For every addition of H_2O_2, there is a linear increase in the cathodic peak current with a slight decrease in the anodic peak current, representing the electrocatalytic reduction of H_2O_2 at the Hb/NIBA-IL/MWCNT/GCE biosensor and the corresponding calibration plot is shown in Fig. 5B. This could be explained with Eq. (2) as described below. On the application of reduction potential to Hb/NIBA-IL/MWCNT/GCE, the reduced Hb-Heme (Fe^{II}) reduces the approaching H_2O_2 into H_2O and is itself oxidised to Hb-Heme (Fe^{III}), which proceeds in a cyclic manner [39]. The inset to Fig. 5A shows both cyclic voltammograms of 0 mM and 3 mM H_2O_2 at the Hb/NIBA-IL/GCE (without MWCNTs). A 50 % decrease in the catalytic current was observed compared to that at a Hb/NIBA-IL/MWCNT/GCE. For comparison, NIBA-IL/MWCNT/GCE was also tested for the electrocatalytic reduction of same concentration of H_2O_2, which showed a feeble current response. The increased current response for the Hb/NIBA-IL/MWCNT/GCE could be ascribed to the stable covalent linking of Hb to NIBA-IL which is π--π stacked over

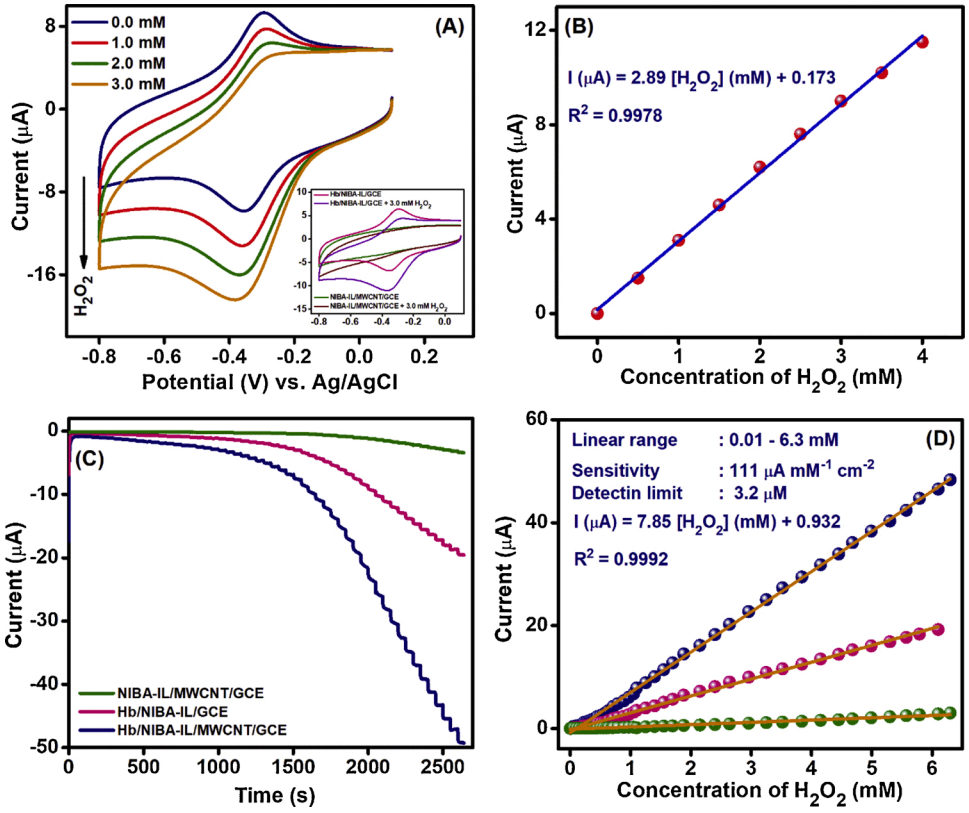

Fig. 5. A) Cyclic voltammograms of 0.0, 1.0, 2.0 and 3.0 mM H_2O_2 at a Hb/NIBA-IL/MWCNT/GCE. Inset: Cyclic voltammograms of 0.0 and 3.0 mM H_2O_2 at a NIBA-IL/MWCNT/GCE and a Hb/NIBA-IL/GCE in 0.1 M phosphate buffer (pH 7.0) at 100 mV s^{-1}. B) Calibration plot for the electrocatalytic reduction of H_2O_2. C) Amperometric i-t curves obtained upon consecutive additions of H_2O_2 at a NIBA-IL/MWCNT/GCE (green), Hb/NIBA-IL/GCE (pink) and a Hb/NIBA-IL/MWCNT/GCE (blue) into a constantly stirred electrolyte. Applied potential: −0.4 V. D) Calibration plots for the determination of H_2O_2.

MWCNT/GCE, which in turn synergistically augmented the electrocatalytic process and yielded better sensitivity to the fabricated biosensor.

$$\text{Hb-Heme } (Fe^{II}) + 2H^{+} + H_2O_2 \rightarrow \text{Hb-Heme } (Fe^{III}) + 2H_2O \quad (2)$$

3.5. Amperometric detection of H_2O_2 at Hb/NIBA-IL/MWCNT/GCE

The electrocatalytic reduction of H_2O_2 by Hb/NIBA-IL/MWCNT/GCE was successfully demonstrated in static conditions, which motivated us to examine the effectiveness of the fabricated biosensor under dynamic conditions. Accordingly, amperometry was performed in a N_2 saturated phosphate buffer (0.1 M, pH 7.0) and the dynamic flow was obtained by continuously stirring the electrolyte using a magnetic stirrer (300 rpm). Initially, the operating potential for the amperometric sensing was optimized by carrying out the measurements at different potentials from −0.3 V to −0.5 V (Fig. S11). Upon increasing the potentials, the current response of Hb/NIBA-IL/MWCNT/GCE towards H_2O_2 determination was also found to increase linearly up to −0.4 V. Beyond −0.40 V, the current response was not linear and consistent and hence −0.40 V was chosen as the optimum potential for amperometric sensing of H_2O_2. Fig. 5C displays the amperometric i–t curve response at an operating potential of −0.4 V for NIBA-IL/MWCNT/GCE, Hb/NIBA-IL/GCE and Hb/NIBA-IL/MWCNT/GCE towards the reduction of different concentrations of H_2O_2. A small current response was obtained at the NIBA-IL/MWCNT/GCE, whereas an immediate increase in the catalytic current was observed for every addition of H_2O_2 to the Hb/NIBA-IL/GCE and Hb/NIBA-IL/MWCNT/GCE system and the response current was observed to stabilise in less than 3 s. Further, the Hb/NIBA-IL/MWCNT/GCE showed a superior sensitivity of 111 μA mM^{-1} cm^{-2}, which is ~2.4 and ~18 times higher than that of Hb/NIBA-IL/GCE (46.3 μA mM^{-1} cm^{-2}) and NIBA-IL/MWCNT/GCE (6.2 μA mM^{-1} cm^{-2}), respectively. The improved sensitivity of Hb/NIBA-IL/MWCNT/GCE is accredited to the electrocatalytic behaviour of Hb facilitated by the synergistic behaviour of NIBA-IL along with the MWCNT modified GCE. Further, the fabricated biosensor showed a linear trend for the concentrations from 0.01 to 6.3 mM with a detection limit of 3.2 μM H_2O_2, which is calculated using the equation 3σ/m, where σ is the standard deviation of blank and m is the slope obtained from the calibration plot (Fig. 5D). The obtained parameters were compared with that of the recently reported Hb biosensors (Table 1) and our results are comparable with the literature reports.

3.6. Stability, reproducibility and interference studies of Hb/NIBA-IL/MWCNT/GCE

Electrocatalytic studies revealed the excellent performance of the fabricated biosensor towards H_2O_2 reduction. Further, the stability of the developed biosensor was investigated in terms of continuous potential cycling as well as reanalyzing the stored biosensor. Fig. 6A shows 50 consecutive cyclic voltammograms of the Hb/NIBA-IL/MWCNT/GCE and the results showed excellent cycling stability without any observable change in the peak behaviour interms of peak currents as well as peak potentials. Inset to Fig. 6A shows the current response obtained periodically for 30 days storage of the fabricated biosensor in the absence and presence of H_2O_2, during which the biosensor retained 96.4 % (absence) and 93.6 % (presence) of its original response. The enhanced cyclic stability and improved storage stability of the developed biosensor could be ascribed to the effective covalent binding of Hb protein on the newly designed NIBA-IL/MWCNT/GCE matrix.

Selectivity is a predominant tool to evaluate the efficacy of any developed biosensors as an analytical tool. Fig. 6B shows the results obtained in a selectivity study on the Hb/NIBA-IL/MWCNT/GCE towards the reduction of 0.4 mM H_2O_2 in the presence of 5-fold excess concentrations of co-existing and commonly interfering analytes including dopamine, uric acid, ascorbic acid, $NaNO_2$, $NaNO_3$, $KClO_3$, glucose, fructose, catechol, glycine, L-cysteine and epinephrine by amperometry. Interestingly, the newly fabricated biosensor showed superior selectivity towards the sensing of H_2O_2 without any observable interference from the co-existing species. The predominant selectivity of the biosensor is likely due to the incorporation of the Hb protein on the NIBA-IL/MWCNT/GCE platform, which selectively identifies the presence of H_2O_2. Further, the reproducibility of the fabricated biosensor was demonstrated by evaluating the performance of five individually fabricated Hb/NIBA-IL/MWCNT/GCEs in the absence and presence of 2 mM H_2O_2. As shown in Fig. S12 the current response obtained for all 5 biosensors yielded a relative standard deviation (RSD) of 1.96 % in the absence and 2.52 % in the presence of H_2O_2, revealing an impressive electrode-to-electrode reproducibility. The superior electrode stability, predominant selectivity and excellent reproducibility of the developed biosensor could be ascribed to the facile fabrication methodology and prodigious properties of the individual components integrated judiciously in the single platform of the NIBA-IL/MWCNT/GCE.

Table 1
Comparison of electrocatalytic performances of various H_2O_2 biosensors.

Electrodes	Linear Range (mM)	Sensitivity(μA mM^{-1} cm^{-2})	LOD (μM)	Ref.
PCS/Hb/CPE	0.1–5	76.43	32.0	[40]
Nafion/Hb/MoS_2/GCE	0.02−0.18	–	6.7	[41]
Hb/AuNPs@MoS_2/GCE	0.01−0.3	–	4	[42]
Nafion/HRP/AuNCs/GCE	0.01–3.27	0.86	0.9	[43]
HRP/GA/PAMAM/CtRGO/GCE	0.05–0.8	29.86	25	[44]
HRP/Sol-gel/MWCNT/GCE	0.07−3.0	–	14.0	[45]
Cyt c/nanoporous Au film	0.01–12.0	2.8	6.3	[46]
Nf/Cyt c-VAErGO/GCE	0.005–2.0	46.3	2.3	[47]
Cyt c/RTIL-PDDA-AuNPs/MUA-MCH/Au	0.04−3.45	–	5.0	[48]
Hb/NIBA-IL/MWCNT/GCE	0.01–6.3	111	3.2	**This work**

AuNCs - Gold nanocomposites; CPE - Carbon paste electrode; CtRGO - Carrot reduced graphene oxide; Cyt C - Cytochrome C; GA - Glutaraldehyde; GCE - Glassy carbon electrode; Hb - Hemoglobin; HRP - Horseradish peroxidase; MUA-MCH - 11-mercaptoundecanoic acid-6-mercapto-1-hexanol; Nf - Nafion; NPs - Nanoparticles; PAMAM - Poly(amidoamine) dendrimer; PCS - PANI/MWCNTs/starch composite material; RTIL-PDDA - Room temperature ionic liquid- Poly (diallyldimethylammonium chloride); VAErGO - Vertically aligned electrochemically reduced graphene oxide.

3.7. Determination of H_2O_2 in real-life samples

The practical applicability of the fabricated biosensor was analyzed by utilizing the Hb/NIBA-IL/MWCNT/GCE biosensor for the estimation of H_2O_2 spiked in the real-life samples of milk and grape juice. The obtained samples were diluted with the phosphate buffer and known concentrations of H_2O_2 were spiked into the electrochemical cell by standard addition method. The results obtained are shown in Fig. S13. The fabricated biosensor displayed good recovery values ranging from 98.4 % to 102.5 % for the determination of H_2O_2 added in the real-life samples (Table 2). Therefore, Hb/NIBA-IL/MWCNT/GCE displays itself as a versatile tool to be used in real-time applications.

4. Conclusion

We report a highly facile and simple biosensor setup for the selective and sensitive determination of H_2O_2. The biosensor consists of a Hb protein covalently attached to a hydrophobic NIBA-IL film over a

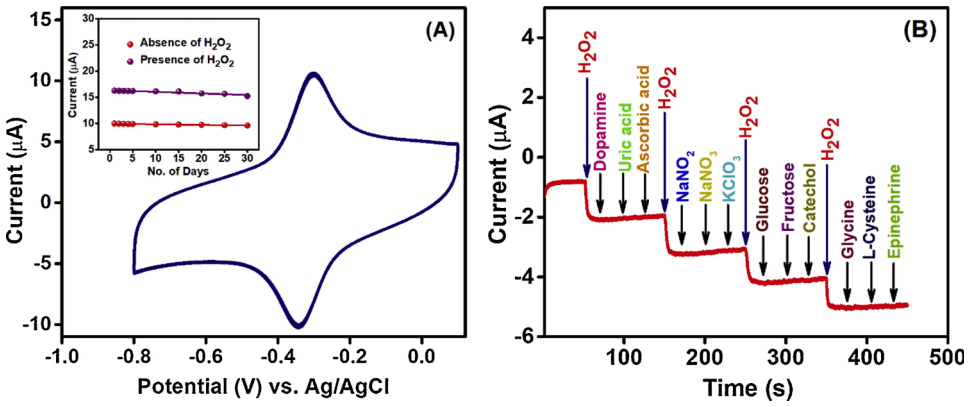

Fig. 6. A) Fifty consecutive cyclic voltammograms of 0.1 M phosphate buffer (pH 7.0) at a Hb/NIBA-IL/MWCNT/GCE (scan rate: 100 mV s^{-1}). Inset: Plot of day-to-day current response for 30 days in the absence (red) and presence (violet) of 2 mM H_2O_2. B) Amperometric response of 0.4 mM H_2O_2 in the presence of 2 mM of various interfering species in 0.1 M phosphate buffer at a Hb/NIBA-IL/MWCNT/GCE (Operating potential: −0.4 V).

Table 2
Determination of H_2O_2 in real samples.

Samples	Spiked (mM)	Found[a] (mM)	Recovery (%)
Milk	0.5	0.492	98.4
	1.0	0.985	98.5
Grape Juice	1.5	1.492	99.4
	2.0	2.051	102.5

[a] Triplicates were performed.

MWCNT/GCE platform. The —COOH group of NIBA-IL and -NH_2 group of Hb were chemically coupled by EDC/NHS cross coupling. On the other hand, naphthyl group of NIBA-IL was employed for π--π stacking over the MWCNT modified GCE. Thus, fabricated Hb/NIBA-IL/MWCNT/GCE showed a well defined redox behaviour corresponding to the deeply buried Fe^{III}/Fe^{II} redox couple of Hb, thereby direct electron transfer of Hb was successfully accomplished. Further, the developed Hb biosensor exhibited an excellent electrocatalytic reduction of H_2O_2 and showed a linear range between 0.01 and 6.3 mM with excellent sensitivity (111 μA mM^{-1} cm^{-2}) and a limit of detection of 3.2 μM. Furthermore, the Hb biosensor showed exceptional stability (50 concecutive cycles) and remarkable electrode-to-electrode (RSD of 2.52 %) reproducibility due to the covalent immobilization of water soluble Hb. On the whole, NIBA-IL/MWCNT/GCE could be used as an efficacious matrix for the development of various biosensors and immunosensors, with enhanced analytical performance and thus making them befitting for diverse analytical applications.

CRediT authorship contribution statement

Manoharan Murphy: Investigation, Methodology, Validation, Writing - original draft. **K. Theyagarajan:** Investigation, Validation, Writing - original draft. **Kathavarayan Thenmozhi:** Conceptualization, Writing - review & editing, Supervision. **Sellappan Senthilkumar:** Conceptualization, Writing - review & editing, Project administration, Supervision.

Declaration of Competing Interest

The authors declare that they have no known competing financial interests or personal relationships that could have appeared to influence the work reported in this paper.

Acknowledgements

Department of Biotechnology (DBT), Ministry of Science & Technology, Government of India (Sanction No. BT/Bio-CARe/05/9784/2013-2014) is gratefully acknowledged for the financial support. The authors also thank the Vellore Institute of Technology (VIT) for providing 'VIT SEED GRANT' for carrying out this research.

Appendix A. Supplementary data

Supplementary material related to this article can be found, in the online version, at doi:https://doi.org/10.1016/j.colsurfb.2020.111540.

References

[1] B. Thirumalraj, C. Rajkumar, S.M. Chen, P. Barathi, Highly stable biomolecule supported by gold nanoparticles/graphene nanocomposite as a sensing platform for H_2O_2 biosensor application, J. Mater. Chem. B 4 (2016) 6335–6343, https://doi.org/10.1039/C6TB01576J.
[2] Y. Li, L. Tang, D. Deng, J. Ye, Z. Wu, J. Wang, L. Luo, A novel non-enzymatic H_2O_2 sensor using $ZnMn_2O_4$ microspheres modified glassy carbon electrode, Colloids Surf., B 179 (2019) 293–298, https://doi.org/10.1016/j.colsurfb.2019.04.008.
[3] T. dos Santos Pereira, G.C.M. de Oliveira, F.A. Santos, P.A. Raymundo-Pereira, O. N. Oliveira Jr, B.C. Janegitz, Use of zein microspheres to anchor carbon black and hemoglobin in electrochemical biosensors to detect hydrogen peroxide in cosmetic products, food and biological fluids, Talanta 194 (2019) 737–744, https://doi.org/10.1016/j.talanta.2018.10.068.
[4] W. Chen, S. Cai, Q.Q. Ren, W. Wen, Y.D. Zhao, Recent advances in electrochemical sensing for hydrogen peroxide: a review, Analyst 137 (2012) 49–58, https://doi.org/10.1039/C1AN15738H.
[5] L. García-Carmona, M. Moreno-Guzmán, A. Martín, S.B. Martínez, A.B. Fernández-Martínez, M.C. González, J. Lucio-Cazaña, A. Escarpa, Aligned copper nanowires as a cut-and-paste exclusive electrochemical transducer for free-enzyme highly selective quantification of intracellular hydrogen peroxide in cisplatin-treated cells, Biosens. Bioelectron. 96 (2017) 146–151, https://doi.org/10.1016/j.bios.2017.04.048.
[6] R. Pinnaratip, P.K. Forooshani, M. Li, Y.H. Hu, R.M. Rajachar, B.P. Lee, Controlling the release of hydrogen peroxide from catechol-based adhesives using silica nanoparticles, ACS Biomater. Sci. Eng. 6 (2020) 4502–4511, https://doi.org/10.1021/acsbiomaterials.0c00572.
[7] A. Khataee, M.H. Irani-nezhad, J. Hassanzadeh, Improved peroxidase mimetic activity of a mixture of WS_2 nanosheets and silver nanoclusters for chemiluminescent quantification of H_2O_2 and glucose, Microchim. Acta 185 (2018) 190, https://doi.org/10.1007/s00604-018-2727-4.
[8] Y. Gao, G. Wang, H. Huang, J. Hu, S.M. Shah, X. Su, Fluorometric method for the determination of hydrogen peroxide and glucose with Fe_3O_4 as catalyst, Talanta 85 (2011) 1075–1080, https://doi.org/10.1016/j.talanta.2011.05.021.
[9] P.A. Raymundo-Pereira, F.M. Shimizu, D. Coelho, M.H.O. Piazzeta, A.L. Gobbi, S.A. S. Machado, O.N. Oliveira Jr., A nanostructured bifunctional platform for sensing of glucose biomarker in artificial saliva: synergy in hybrid Pt/Au surfaces, Biosens. Bioelectron. 86 (2016) 369–376, https://doi.org/10.1016/j.bios.2016.06.053.
[10] M.P. Gimeno, M.C. Mayoral, J.M. Andres, A potentiometric titration for H_2O_2 determination in the presence of organic compounds, Anal. Methods 5 (2013) 1510–1514, https://doi.org/10.1039/C3AY26329K.
[11] P. Gimeno, C. Bousquet, N. Lassu, A.F. Maggio, C. Civade, C. Brenier, L. Lempereur, High-performance liquid chromatography method for the determination of hydrogen peroxide present or released in teeth bleaching kits and hair cosmetic products, J. Pharm. Biomed. Anal. 107 (2015) 386–393, https://doi.org/10.1016/j.jpba.2015.01.018.
[12] P.A. Raymundo-Pereira, M. Baccarin, O.N. Oliveira Jr, B.C. Janegitz, Thin films and composites based on graphene for electrochemical detection of biologically-

relevant molecules, Electroanalysis 30 (2018) 1888–1896, https://doi.org/10.1002/elan.201800283.
[13] D. Ye, Y. Xu, L. Luo, Y. Ding, Y. Wang, X. Liu, L. Xing, J. Peng, A novel nonenzymatic hydrogen peroxide sensor based on $LaNi_{0.5}Ti_{0.5}O_3/CoFe_2O_4$ modified electrode, Colloids Surf., B 89 (2012) 10–14, https://doi.org/10.1016/j.colsurfb.2011.08.014.
[14] M.F.S. Teixeira, F.H. Cincotto, P.A. Raymundo-Pereira, Electrochemical investigation of the dimeric oxo-bridged ruthenium complex in aqueous solution and its incorporation within a cation-exchange polymeric film on the electrode surface for electrocatalytic activity of hydrogen peroxide oxidation, Electrochim. Acta 56 (2011) 6804–6811, https://doi.org/10.1016/j.electacta.2011.05.085.
[15] T. Marimuthu, M.R. Mahmoudian, S. Mohamad, Y. Alias, Synthesis and characterization of non-enzymatic hydrogen peroxide sensor of polypyrrole coated nanocomposites, Sens. Actuators, B 202 (2014) 1037–1043, https://doi.org/10.1016/j.snb.2014.06.044.
[16] B. Wang, L. Luo, Y. Ding, D. Zhao, Q. Zhang, Synthesis of hollow copper oxide by electrospinning and its application as a nonenzymatic hydrogen peroxide sensor, Colloids Surf., B 97 (2012) 51–56, https://doi.org/10.1016/j.colsurfb.2012.03.013.
[17] J. Yoon, T. Lee, G.B. Bapurao, J. Jo, B.K. Oh, J.W. Choi, Electrochemical H_2O_2 biosensor composed of myoglobin on MoS_2 nanoparticle-graphene oxide hybrid structure, Biosens. Bioelectron. 93 (2017) 14–20, https://doi.org/10.1016/j.bios.2016.11.064.
[18] S.E. Salamifar, S. Lee, R.Y. Lai, Electrochemical hydrogen peroxide sensors fabricated using cytochrome *c* immobilized on macroelectrodes and ultramicroelectrodes, Colloids Surf., B 123 (2014) 866–869, https://doi.org/10.1016/j.colsurfb.2014.10.033.
[19] K. Thenmozhi, S.S. Narayanan, Horseradish peroxidase and toluidine blue covalently immobilized leak-free sol-gel composite biosensor for hydrogen peroxide, Mater. Sci. Eng. C 70 (2017) 223–230, https://doi.org/10.1016/j.msec.2016.08.075.
[20] Y. Wang, J. Du, Y. Li, D. Shan, X. Zhou, Z. Xue, X. Lu, A amperometric biosensor for hydrogen peroxide by adsorption of horseradish peroxidase onto single-walled carbon nanotubes, Colloids Surf., B 90 (2012) 62–67, https://doi.org/10.1016/j.colsurfb.2011.09.045.
[21] R. Del Cano, L. Mateus, G. Sanchez-Obrero, J.M. Sevilla, R. Madueno, M. Blazquez, T. Pineda, Hemoglobin becomes electroactive upon interaction with surface-protected Au nanoparticles, Talanta 176 (2018) 667–673, https://doi.org/10.1016/j.talanta.2017.08.090.
[22] M.J.A. Shiddiky, A.A.J. Torriero, Applications of ionic liquids in electrochemical sensing systems, Biosens. Bioelectron. 26 (2011) 1775–1787, https://doi.org/10.1016/j.bios.2010.08.064.
[23] K. Kwak, S. Senthilkumar, K. Pyo, D. Lee, Ionic liquid of a gold nanocluster: a versatile matrix for electrochemical biosensors, ACS Nano 8 (2014) 671–679, https://doi.org/10.1021/nn4053217.
[24] Y. Fan, D. Zhang, J. Wang, H. Jin, Y. Zhou, D. Yan, Preparation of anion-exchangeable polymer vesicles through the self-assembly of hyperbranched polymeric ionic liquids, Chem. Commun. 51 (2015) 7234–7237, https://doi.org/10.1039/C5CC01802A.
[25] Z.L. Hou, T. Huang, C.Y. Cai, T. Resheed, C.Y. Yu, Y.F. Zhou, D.Y. Yan, Polymer vesicle sensor through the self-assembly of hyperbranched polymeric ionic liquids for the detection of SO_2 derivatives, Chin. J. Polym. Sci. 35 (2017) 602–610, https://doi.org/10.1007/s10118-017-1921-x.
[26] C. Yue, D. Fang, L. Liu, T.F. Yi, Synthesis and application of task-specific ionic liquids used as catalysts and/or solvents in organic unit reactions, J. Mol. Liq. 163 (2011) 99–121, https://doi.org/10.1016/j.molliq.2011.09.001.
[27] W.H. Zhang, P.P. He, S. Wu, J. Xu, Y. Li, G. Zhang, X.Y. Wei, Graphene oxide grafted hydroxyl-functionalized ionic liquid: a highly efficient catalyst for cycloaddition of CO_2 with epoxides, Appl. Catal. A 509 (2016) 111–117, https://doi.org/10.1016/j.apcata.2015.10.038.
[28] W. Chen-Feng, S. Xin-Yue, S. Ming, W. Yi-Peng, L. Yun-Kai, Electrochemical biosensors based on antibody, nucleic acid and enzyme functionalized graphene for the detection of disease-related biomolecules, Analyst 145 (2020) 1550–1562, https://doi.org/10.1039/C9AN02047K.
[29] M. Murphy, K. Theyagarajan, G. Prabusankar, S. Senthilkumar, K. Thenmozhi, Electrochemical biosensor for the detection of hydrogen peroxide using cytochrome *c* covalently immobilized on carboxyl functionalized ionic liquid/multiwalled carbon nanotube hybrid, App. Surf. Sci. 492 (2019) 718–725, https://doi.org/10.1016/j.apsusc.2019.06.283.
[30] M. Roushani, K. Bakyas, B.Z. Dizajdizi, Development of sensitive amperometric hydrogen peroxide sensor using a CuNPs/MB/MWCNT-C_{60}-Cs-IL nanocomposite modified glassy carbon electrode, Mater. Sci. Eng. C 64 (2016) 54–60, https://doi.org/10.1016/j.msec.2016.03.078.
[31] N. Xia, Y. Xing, G. Wang, Q. Feng, Q. Chen, H. Feng, X. Sun, L. Liu, Probing of EDC/NHSS-mediated covalent coupling reaction by the immobilization of electrochemically active biomolecules, Int. J. Electrochem. Sci. 8 (2013) 2459–2467.
[32] P.N. Muskawar, S. Senthilkumar, P.R. Bhagat, Carboxyl-functionalized ionic liquids based on Benzimidazolium cation: study of Hammett values and catalytic activity towards one-pot synthesis of 1-amidoalkyl naphthols, J. Mol. Catal. A Chem. 380 (2013) 112–117, https://doi.org/10.1016/j.molcata.2013.09.026.
[33] P.N. Muskawar, K. Thenmozhi, J.M. Gajbhiye, P.R. Bhagat, Facile esterification of carboxylic acid using amide functionalized benzimidazolium dicationic ionic liquids, Appl. Catal. A Gen. 482 (2014) 214–220, https://doi.org/10.1016/j.apcata.2014.06.004.
[34] N.N. Al-Mohammed, R.S. Duali Hussen, Y. Alias, Z. Abdullah, Tris-imidazolium and benzimidazolium ionic liquids: a new class of biodegradable surfactants, RSC Adv. 5 (2015) 2869–2881, https://doi.org/10.1039/c4ra14027c.
[35] W. Sun, Y. Guo, X. Ju, Y. Zhang, X. Wang, Z. Sun, Direct electrochemistry of hemoglobin on graphene and titanium dioxide nanorods composite modified electrode and its electrocatalysis, Biosens. Bioelectron. 42 (2013) 207–213, https://doi.org/10.1016/j.bios.2012.10.034.
[36] K. Theyagarajan, D. Saravanakumar, S. Senthilkumar, K. Thenmozhi, Rationally designed naphthyl substituted amine functionalized ionic liquid platform for covalent immobilization and direct electrochemistry of hemoglobin, Sci. Rep. 9 (2019) 10428, https://doi.org/10.1038/s41598-019-46982-3.
[37] J. Li, J. Tang, L. Zhou, X. Han, H. Liu, Direct electrochemistry and electrocatalysis of hemoglobin immobilized on polyacrylamide-P123 film modified glassy carbon electrode, Bioelectrochemistry 86 (2012) 60–66, https://doi.org/10.1016/j.bioelechem.2012.02.002.
[38] Y. Wen, W. Wen, X. Zhang, S. Wang, Highly sensitive amperometric biosensor based on electrochemically-reduced graphene oxide-chitosan/hemoglobin nanocomposite for nitromethane determination, Biosens. Bioelectron. 79 (2016) 894–900, https://doi.org/10.1016/j.bios.2016.01.028.
[39] A.T.E. Vilian, S.M. Chen, C.H. Kwak, S.K. Hwang, Y.S. Huh, Y.K. Han, Immobilization of hemoglobin on functionalized multi-walled carbon nanotubes-poly-L-histidine-zinc oxide nanocomposites toward the detection of bromate and H_2O_2, Sens. Actuators, B 224 (2016) 607–617, https://doi.org/10.1016/j.snb.2015.10.099.
[40] V. Gautam, K.P. Singh, V.L. Yadav, Polyaniline/multiwall carbon nanotubes/starch nanocomposite material and hemoglobin modified carbon paste electrode for hydrogen peroxide and glucose biosensing, Int. J. Biol. Macromol. 111 (2018) 1124–1132, https://doi.org/10.1016/j.ijbiomac.2018.01.094.
[41] H. Liu, X. Su, C. Duan, X. Dong, Z. Zhu, A novel hydrogen peroxide biosensor based on immobilized hemoglobin in 3D flower-like MoS_2 microspheres structure, Mater. Lett. 122 (2014) 182–185, https://doi.org/10.1016/j.matlet.2014.02.047.
[42] J. Chao, M. Zou, C. Zhang, H. Sun, D. Pan, H. Pei, S. Su, L. Yuwen, C. Fan, L. Wang, A MoS_2-based system for efficient immobilization of hemoglobin and biosensing applications, Nanotechnology 26 (2015) 274005, https://doi.org/10.1088/0957-484/26/27/274005.
[43] H. Fang, Q. Xiaoli, B. Lijuan, F. Yingchun, T. Yueming, C. Chao, L. Yunlong, X. Qingji, Y. Shouzhuo, Study on the bioelectrochemistry of a horseradish peroxidase-gold nanoclusters bionanocomposite, J. Electroanal. Chem. 792 (2017) 39–45, https://doi.org/10.1016/j.jelechem.2017.03.033.
[44] C.S.R. Vusa, V. Manju, S. Berchmans, P. Arumugam, Electrochemical amination of graphene using nanosized PAMAM dendrimers for sensing applications, RSC Adv. 6 (2016) 33409–33418, https://doi.org/10.1039/C5RA27862G.
[45] S.X. Xu, J.L. Li, Z.L. Zhou, C.X. Zhang, A third-generation hydrogen peroxide biosensor based on horseradish peroxidase immobilized by sol-gel thin film on a multi-wall carbon nanotube modified electrode, Anal. Methods 6 (2014) 6310–6315, https://doi.org/10.1039/C4AY00541D.
[46] A. Zhu, Y. Tian, H. Liu, Y. Luo, Nanoporous gold film encapsulating cytochrome c for the fabrication of a H_2O_2 biosensor, Biomaterials 30 (2009) 3183–3188, https://doi.org/10.1016/j.biomaterials.2009.02.019.
[47] D. Thirumalai, V. Kathiresan, J. Lee, S.H. Jin, S.C. Chang, Electrochemical reactive oxygen species detection by cytochrome c immobilized with vertically aligned and electrochemically reduced graphene oxide on a glassy carbon electrode, Analyst 142 (2017) 4544–4552, https://doi.org/10.1039/C7AN01387F.
[48] Y. Song, H. Liu, L. Wan, Y. Wang, H. Hou, L. Wang, Direct electrochemistry of cytochrome c based on poly(diallyldimethylammonium chloride)-graphene nanosheets/ gold nanoparticles hybrid nanocomposites and its biosensing, Electroanalysis 25 (2013) 1400–1409, https://doi.org/10.1002/elan.201200524.